



King's Research Portal

DOI:

[10.1002/chem.201803493](https://doi.org/10.1002/chem.201803493)

Document Version

Peer reviewed version

[Link to publication record in King's Research Portal](#)

Citation for published version (APA):

Peña, I., Sanz, M. E., Alonso, E. R., & Alonso, J. L. (2018). The Multiple Hydrogen Bonding Networks of the Polyol Ribitol. *CHEMISTRY*, 24(51), 13408-13412. <https://doi.org/10.1002/chem.201803493>

Citing this paper

Please note that where the full-text provided on King's Research Portal is the Author Accepted Manuscript or Post-Print version this may differ from the final Published version. If citing, it is advised that you check and use the publisher's definitive version for pagination, volume/issue, and date of publication details. And where the final published version is provided on the Research Portal, if citing you are again advised to check the publisher's website for any subsequent corrections.

General rights

Copyright and moral rights for the publications made accessible in the Research Portal are retained by the authors and/or other copyright owners and it is a condition of accessing publications that users recognize and abide by the legal requirements associated with these rights.

- Users may download and print one copy of any publication from the Research Portal for the purpose of private study or research.
- You may not further distribute the material or use it for any profit-making activity or commercial gain
- You may freely distribute the URL identifying the publication in the Research Portal

Take down policy

If you believe that this document breaches copyright please contact librarypure@kcl.ac.uk providing details, and we will remove access to the work immediately and investigate your claim.

CHEMISTRY

A European Journal

A Journal of



Accepted Article

Title: The Multiple Hydrogen Bonding Networks of the Polyol Ribitol

Authors: Isabel Peña, Maria Eugenia Sanz, Elena Rita Alonso, and
Jose Luis Alonso

This manuscript has been accepted after peer review and appears as an Accepted Article online prior to editing, proofing, and formal publication of the final Version of Record (VoR). This work is currently citable by using the Digital Object Identifier (DOI) given below. The VoR will be published online in Early View as soon as possible and may be different to this Accepted Article as a result of editing. Readers should obtain the VoR from the journal website shown below when it is published to ensure accuracy of information. The authors are responsible for the content of this Accepted Article.

To be cited as: *Chem. Eur. J.* 10.1002/chem.201803493

Link to VoR: <http://dx.doi.org/10.1002/chem.201803493>

Supported by
ACES

WILEY-VCH

The Multiple Hydrogen Bonding Networks of the Polyol Ribitol

Isabel Peña, M. Eugenia Sanz,* Elena R. Alonso, and José L. Alonso

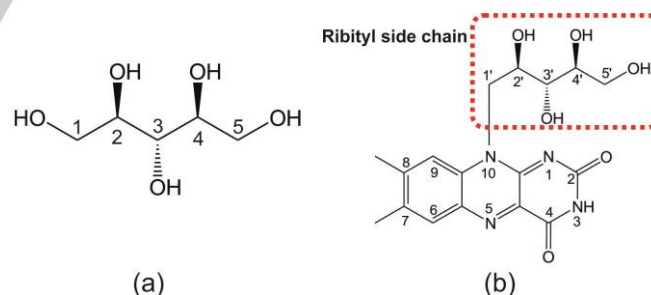
Abstract: Conformational flexibility and non-covalent interactions determine the structure and activity of molecules in biological processes. In this work, the hydrogen bonding networks of the polyol ribitol have been determined for the first time using a combination of laser ablation and broadband rotational spectroscopy. Five conformations of ribitol have been identified, two with extended carbon chains and three with bent chains. All conformations are stabilized by sequential hydrogen bonding networks of either four or five intramolecular O–H...O bonds in a clockwise or counter-clockwise arrangement. The hydrogen bonding patterns are related to the extended or bent-chain conformations of ribitol, and involve 2OH-4OH or 2OH-5OH linkages, respectively. Interestingly, all hydrogen bonds wrap round the carbon backbone of ribitol rather than being located above or below it as it happens for other polyols and cyclic sugars.

Polyols, also known as sugar alcohols or alditols, are polyhydroxylated molecules that participate in a myriad of biological processes, from metabolic reactions to protein structure stabilization and cryopreservation.^[1–3] Polyols are aliphatic, with multiple vicinal hydroxyl groups which can act both as proton donors and acceptors. In this, they are similar to water, and their capacity to form hydrogen bonds with water and disrupt water's hydrogen bonding networks has been proposed as the reason for the role of polyols as stabilisers of protein conformation^[4]. Understanding the biological activity of polyols requires understanding their intermolecular interactions, which are determined by the topology of the polyol and the environment. Therefore knowledge of polyols' bioactivity involves first the atomic-scale determination of their conformations and the intramolecular hydrogen bonding patterns that dictate them.

The high flexibility of polyols has prevented a detailed knowledge of their intrinsic conformations. Their studies in condensed phases have returned either the frozen conformation in the solid, or hints of a conformational ensemble in the liquid that could not be disentangled.^[5,6] A high resolution spectroscopic technique capable of resolving the individual conformational signatures without interference from the media should be applied. Furthermore, polyols are solids at room temperature, and require a suitable vaporization method for their

transfer to the gas phase without decomposition. These two challenges have been solved with the use of broadband rotational spectroscopy^[7] in combination with laser ablation, using a laser ablation chirped pulse Fourier transform microwave (LA-CP-FTMW) spectrometer.^[8,9] Rotational spectroscopy had been applied to vicinal diols and glycerol (a triol), which can be vaporized by heating.^[10–17] LA-CP-FTMW has proved successful in recent works to elucidate the intramolecular interactions in serinol, the polar headgroup of the lipid sphingosine, and other important biomolecules.^[18–20]

In this work we have focused on one of the naturally occurring five-carbon polyols, ribitol (C₅H₁₂O₅, also known as adonitol, see Scheme 1), which is formed by the reduction of ribose. Ribitol has been chosen as it has properties that set it slightly apart from other polyols. Rather than being used as a sweetener, it forms part of the cell walls of Gram positive bacteria^[21] and constitutes the flexible tail of riboflavin (Scheme 1). The ribityl tail of flavins has been proved to exert crucial catalytic activity in several flavoproteins^[22–24] through the 2'OH site, and to act as a flexible switch controlling protein-membrane binding^[24]. Ribitol has been studied in the crystal,^[25] where one conformation with a bent carbon chain was observed, and in solution, where it was found that several conformations coexist, but they could not be identified.^[6] Understanding the factors that lead ribitol to exist as a conformational ensemble or as a unique structure requires characterization of its intrinsic conformational preferences. Then the role of the environment, and any structural changes occurring upon interactions with surrounding molecules, could be assessed.



Scheme 1. Molecular structure of (a) ribitol and (b) riboflavin.

The broadband rotational spectrum of ribitol (see Fig. 1) is quite crowded, showing a large number of lines. Identification of spectral patterns corresponding to different conformations is achieved by comparison with predictions from theory. The very flexible nature of ribitol required us to conduct an extensive conformational search, first using the AM1 method^[26] varying all torsional angles of ribitol, and subsequently optimizing the AM1 conformational minima at MP2 level. This yielded 44 structures below 25 kJmol⁻¹. The lower-energy ones are mostly grouped in TG and TT families according to the configuration of the two

[*] Dr. I. Peña, Dr. M. E. Sanz
Department of Chemistry
King's College London
London SE1 1DB, United Kingdom
E-mail: maria.sanz@kcl.ac.uk
Dr. I. Peña, E. Alonso, Prof. J. L. Alonso
Grupo de Espectroscopia Molecular (GEM)
Edificio Quifima, Laboratorio de Espectroscopia y Bioespectroscopia
Unidad Asociada CSIC, Parque Científico Uva
Universidad de Valladolid, 47011 Valladolid (Spain)

Supporting information for this article is given via a link at the end of the document.

COMMUNICATION

WILEY-VCH

dihedral angles $\angle C_1C_2C_3C_4$ and $\angle C_2C_3C_4C_5$. The configuration of the oxygen atoms of the OH groups is indicated by the g+,g- and t labels of the corresponding values of $+60^\circ$, -60° and 180° of the 4 dihedral angles $\angle O_1C_1C_2O_2$, $\angle O_2C_2C_3O_3$, $\angle O_3C_3C_4O_4$, and $\angle O_4C_4C_5O_5$, and the clockwise (cw) or counterclockwise (cc) direction of the hydrogen bonding network is indicated by the corresponding prefix. A further numeral label indicates differences in the hydrogen atom arrangements. Spectral

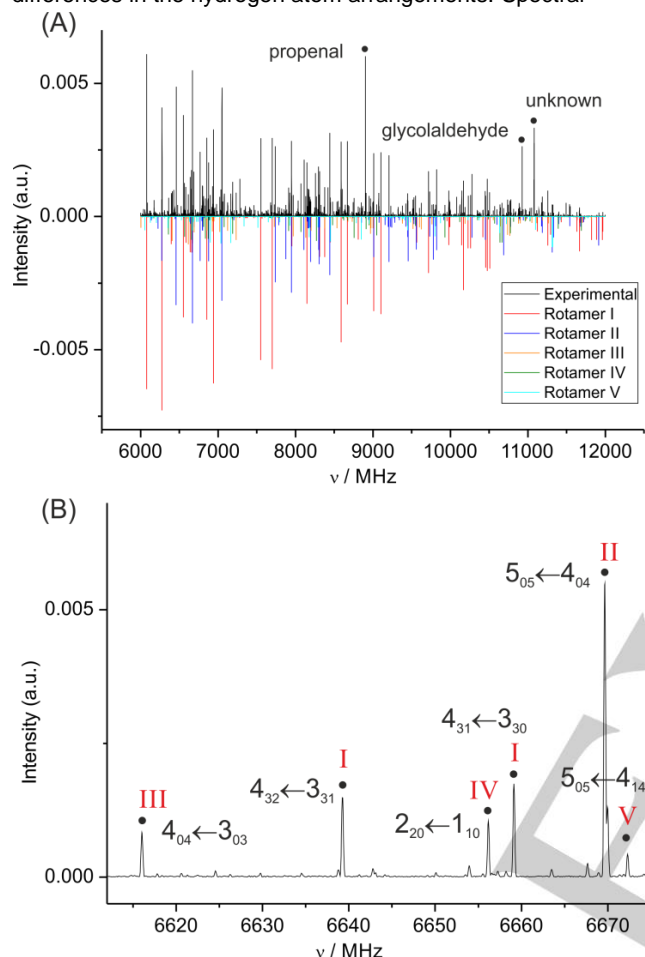


Figure 1. (A) Broadband rotational spectrum of D-ribose in the 6-12 GHz frequency range. The upper trace shows the experimental spectrum, the lower trace is a simulation with the fitted rotational parameters. (B) An expanded view of the spectrum showing some of the rotational transitions ascribed to the five detected rotamers.

searches focused on finding the typical patterns of a -type $J + 1 \leftarrow J$ rotational transitions, predicted to be observable for the lower-lying energy conformations (see Table 1). Five rotamers were identified, with rotamers I and II dominating the spectrum

and rotamers III, IV and V showing weaker a -type progressions. Experimental rotational and centrifugal distortion constants (see Table 2) were obtained by fitting the Watson Hamiltonian in the A reduction and I' representation^[27] to the measured transitions (see Tables S1-S5 of the Sup. Inf.) using Pickett's program.^[28]

Identification of the observed conformers is achieved by comparing the experimental values of the spectroscopic parameters (Table 2) with those predicted ab initio (Table 1). The different mass distribution of the conformers is reflected in the values of their rotational constants. Thus a first assessment of the rotational constants indicates that rotamers I, III and IV have bent carbon backbones belonging to the TG family, while conformers II and V have completely extended carbon chains and belong to the TT family (see figures in Table 1). A further look into the experimental rotational constants allows identification of rotamers II and V as conformers cw-TT/g-ttg- and cw-TT/g-ttg+, respectively. Rotamers III and IV are assigned as conformers cw-TG/g-tg+g- and cc-TG/g-tg+g+, respectively, by considering their rotational constants and theoretical dipole moment components together with their observed transitions (a - and b - type transitions for rotamer III and a - and c - type transitions for rotamer IV). The rotational constants of rotamer I and its observed transitions match those of conformers cc-TG/g-tg+g+1 and cc-TG/g-tg+g+2. Rotamer I was assigned to conformer cc-TG/g-tg+g+1 on the basis of its lower predicted energy and relaxation of conformer cc-TG/g-tg+g+2 to conformer cc-TG/g-tg+g+1 (see Figure S1 of the Sup. Inf.).

Experimental conformational abundances were estimated from relative intensity measurements of common transitions, considering that intensity of rotational transitions is proportional to conformer number density multiplied by the square of the corresponding dipole moment component, $N_i \cdot \mu_i^2$. Using the theoretical values of the dipole moment components of Table 1, it was found that conformer cc-TG/g-tg+g+1 is the least abundant conformer, followed by conformer cw-TG/g-tg+g+. The other observed conformers are more abundant, but their estimated relative abundances are not consistent when considering different transition types, and it is not possible to establish their abundance ordering. Line intensity depends on the square of the corresponding dipole moment component, which determines the optimum power for polarisation. Because ribitol molecules are polarised at fixed power in our experiment, it is possible that lines associated with very different values of the dipole moment components (see Table 2) are not all optimally polarised, and this can cause discrepancies in the evaluation of relative abundances.

Table 1. Ab initio^[a] spectroscopic parameters for the predicted conformers of ribitol with energies within 10 kJ/mol.

Parameter	cw-TG/g-tg+g+	cc-TG/g-tg+g+	cc-TG/g-tg+g+1	cc-TG/g-tg+g+2	cw-TT/g-ttg-	cw-TG/g-tg+g+	cw-TT/g-ttg+
$A^{[b]}$ (MHz)	1982.2	1974.7	1886.9	1889.3	2522.2	1863.5	2114.2
B (MHz)	975.4	971.2	941.9	933.7	739.8	943.8	842.7
C (MHz)	761.1	758.1	716.8	712.8	621.2	719.4	710.5
μ_a (D)	0.7	-0.6	2.9	1.5	-1.5	-2.0	-0.3
μ_b (D)	0.6	0.2	-0.2	-0.3	-0.5	1.9	-0.8
μ_c (D)	-0.2	-0.7	-1.2	0.5	-1.0	-1.5	-0.2
$\Delta E_{MP2}^{[c]}$ (kJ mol ⁻¹)	0.0	3.15	3.57	5.63	8.17	8.92	9.86
$\Delta E_{MP2+7PC}^{[d]}$ (kJ mol ⁻¹)	0.0	3.52	3.64	5.61	6.32	8.13	8.72
$\Delta G^{298[e]}$ (kJ mol ⁻¹)	0.0	3.35	3.86	5.71	4.36	8.01	5.66

[a] MP2/6-311++G(d,p); [b] A , B , C are the rotational constants; μ_a , μ_b and μ_c are the electric dipole moment components; [c] Relative electronic energies; [d] Relative electronic energies including the zero-point correction; [e] Gibbs free energies at 298 K calculated at the MP2/6-311++G(d,p) level.

Table 2. Experimental rotational parameters for the five observed conformers of ribitol.

Parameter	Rotamer I	Rotamer II	Rotamer III	Rotamer IV	Rotamer V
$A^{[a]}$ (MHz)	1883.71449(48) ^[e]	2522.99272(44)	1978.04651(79)	1959.04993(59)	2110.21884(77)
B (MHz)	932.96871(25)	737.49183(18)	965.16834(32)	959.75717(30)	826.21822(30)
C (MHz)	711.96560(31)	618.62760(20)	755.08283(38)	749.09597(45)	706.88440(33)
Δ_J (kHz)	0.0410(29)	0.0238(16)	0.0503(41)	0.0362(50)	0.0686(37)
Δ_{JK} (kHz)	0.172(19)	0.0466(43)	0.274(17)	0.516(19)	0.114(29)
$a/b/c^{[b]}$	y/n/y	y/y/y	y/y/n	y/n/y	y/y/n
$N^{[c]}$	43	66	46	41	43
$\sigma^{[d]}$ (kHz)	4.8	4.5	6.4	5.7	6.1

[a] A , B , C are the rotational constants; Δ_J and Δ_{JK} are the centrifugal distortion constants. [b] Yes (y) or no (n) observation of a -, b - and c -type transitions. [c] Number of fitted transitions. [d] rms deviation of the fit. [e] Standard error in parentheses in units of the last digit.

The theoretical conformational abundances calculated from Gibbs free energies at 298 K, assuming thermal equilibration in our laser plume, are not in agreement with our experimental results, as they predict TT conformers to be the least abundant. In our estimation we have not considered conformational relaxation in the supersonic expansion from higher energy conformers to lower energy ones. However, it is not possible to entirely disregard its occurrence (Ne was used as a carrier gas), and so our results must be considered with caution. It may also be necessary to use a higher level of theory to predict more accurately the conformational abundances of ribitol. Nonetheless, the five conformations of ribitol predicted to be most abundant at MP2 level have been observed in our experiment.

Several conclusions can be derived from our observations. All identified conformers (Fig. 2) are stabilized by chains of 4 or 5 hydrogen bonds, with different hydrogen bonding patterns depending on the carbon chain configuration. TT conformers with extended carbon backbones present the $O_1H \leftrightarrow O_2H \leftrightarrow O_4H \leftrightarrow O_5H \leftrightarrow O_3H \leftrightarrow O_1$ hydrogen bonding network, while TG conformers with bent carbon chains show $O_1H \leftrightarrow O_2H \leftrightarrow O_5H \leftrightarrow O_4H \leftrightarrow O_3H \leftrightarrow O_1$ linkages. Hence in ribitol it is possible to predict hydrogen bond interactions from the

conformation of the carbon chain. Interestingly, the hydrogen bonding networks in ribitol wrap around the carbon backbone rather than being preferentially located above or below it as it happens for polyols like sorbitol and dulcitol^[29] and cyclic sugars like ribose^[30] and glucose^[31]. This different arrangement of the hydrogen bonding networks may be what confers ribitol its distinctive bioactivity with respect to other polyols.

From our data it is possible to determine not only the bonding pattern but also the directionality of the hydrogen bonding chain. The ribitol conformers present sequential or homodromic (in the same direction) chains, either in the clockwise (cw) or counter-clockwise (cc) direction. This type of hydrogen bonding is associated with enhanced hydrogen bond cooperativity,^[32,33] as polarization of the chains strengthens hydrogen bonds and increases the hydrogen bond energy. In comparison with five- and six-membered cyclic ribose,^[30,34] the longer chains of hydrogen bonds of ribitol and the lack of a hemiacetal oxygen acting as a chain stopper are likely to result in stronger hydrogen bond cooperativity. In fact, ribitol has generally shorter $O-H \cdots O$ hydrogen bonds, ranging 1.8–2.6 Å if the theoretical bond lengths of ribitol conformers are taken as good descriptions of the actual ones (which is granted by the small differences between theoretical and experimental

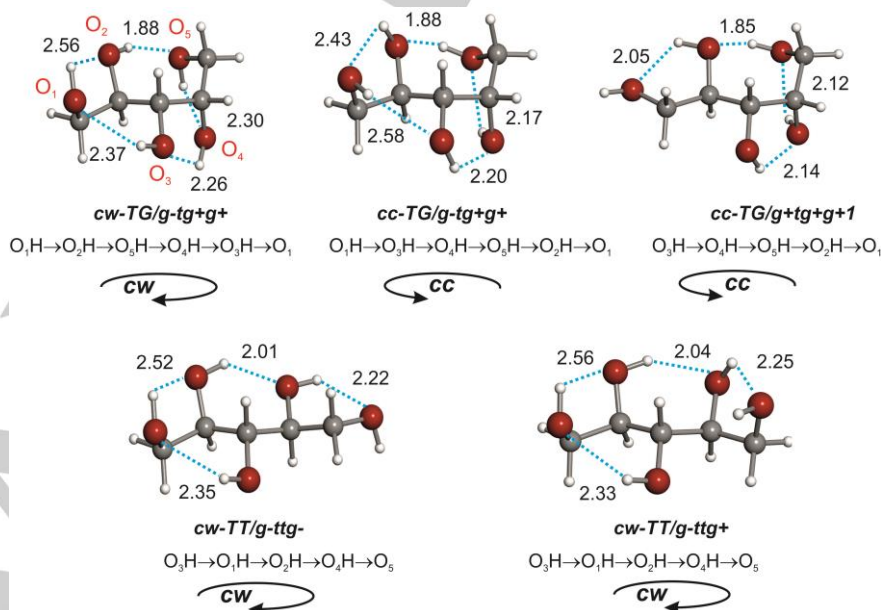


Figure 2. The five observed conformers of ribitol showing the intramolecular hydrogen bond distances in Å and the clockwise (cw) and counterclockwise (cc) orientation of the hydroxyl groups.

COMMUNICATION

WILEY-VCH

rotational constants, lower than 1% on average).

The shortest hydrogen bond in all ribitol conformers is established between $O_2H \leftrightarrow O_5H$ (TG conformers) or $O_2H \leftrightarrow O_4H$ (TT conformers), with values of 1.9 Å and 2.0 Å, respectively (Fig. 2). This is consistent with cooperativity expectations that the largest cooperativity effects will occur in the hydrogen bonds in the middle of the chain. Remarkably, conformer cc-TG/g+tg+g+1 displays the shortest hydrogen bonds, all 1.8–2.1 Å. Shorter hydrogen bonds are usually associated with stronger interactions.^[32,33] Since conformer cc-TG/g+tg+g+1 is the least abundant conformer, this finding points to other effects acting as conformational determinants in addition to hydrogen bonding, such as hyperconjugative effects.

The identification of the conformations of ribitol in the gas phase allows us to gauge the effect of the environment on conformational behavior by comparing the gas phase data with that obtained in condensed phases and in proteins. Ribitol displays only one conformation in the crystal, a bent chain with one kink in the carbon backbone^[25] that it is predicted to lie at ca. 1300 cm⁻¹ (15 kJ/mol) above the global minimum (see Table S6 of Sup. Inf.). It was speculated that selection of this structure in the crystal was due to intramolecular hydrogen bonding in ribitol and to minimize repulsive interactions,^[25] but our data shows that it is due to the influence of intermolecular hydrogen bonds and molecular packing forces in the solid phase. In solution^[6] several conformations were found to coexist, but their structures could not be identified. In flavin proteins where the ribityl chain has been reported to be vital for catalysis,^[22–24] the chain adopts an extended conformation with 2'OH–4'OH contacts like those reported here for the TT conformers (see Fig. S2 in the Sup. Inf.). These results show that the environment impacts strongly on ribitol conformational behavior. Further investigations at the molecular level are necessary to assess how interactions of ribitol with other molecules, including ribitol itself, water and mimics of proteins residues affect its conformational preferences. Most of the observed conformations of ribitol are predicted low overall dipole moments resulting from the partial cancellation of bond dipole moments due to the cyclic arrangement of hydrogen bonds. Conformations cc-TG/g+tg+g+1 and cw-TT/g-ttg- present the largest dipole moments and have a terminal hydrogen atom pointing outwards. Would this make them more susceptible of interacting with other molecules? Would differences in polarity between the different conformers have a significant effect in binding energies and structural preferences of the complexes?

In summary, the topology of ribitol has been revealed in the gas phase to consist of a mixture of five conformations with extended and bent chains. The hydrogen bonding networks of all conformers are formed by chains of four or five cyclic sequential O–H...O bonds and their directionality (cc or cw) has been resolved. The latter is thought to be important in carbohydrate recognition, and together with the wrap-around configuration of the hydrogen bond networks (forgoing the existence of hydrophilic and hydrophobic sides in ribitol), presumably affect polyol interactions with water and other biological molecules. The results presented here can be taken as a basis to study ribitol's self-assembly and interactions with water, which can shed light on its behaviour in the crystal, and in solution as protein stabiliser. Mimicking (partially or totally) the possible interactions of ribityl side chain in flavins can provide clues as to its catalytic role, and supplement X-ray data where resolution better than 2 Å is usually difficult to achieve. Gas phase data, with its direct benchmarking of theory, complements

other techniques and helps develop fundamental insight into the structural choices of biological molecules.

Experimental Section

A commercial sample of D-ribitol (m.p. 102–105 °C) was vaporized using the fourth (266 nm) harmonic of a 20 picosecond Nd:YAG laser (10 mJ per pulse) and conducted by a flow of Ne at ca. 15 bar to expand adiabatically into the vacuum chamber and be probed by broadband CP-FTMW.^[8,9] An arbitrary waveform generator created a chirped microwave pulse that linearly swept the entire 6–12 GHz frequency region and was amplified by a travelling wave tube amplifier with 300 W maximum output power. The amplified pulse was broadcast into the vacuum chamber through two microwave horns and polarised the vaporized molecules in the pulsed jet. Molecular free induction decay signals (FIDs) were amplified and digitized on a fast oscilloscope. A total of 127000 averages at 2 Hz repetition rate were averaged in the time domain and Fourier transformed to obtain the rotational spectra in the 6 to 12 GHz frequency range (see Figure 1).

Acknowledgements

This work was supported by the EU FP7 (Marie Curie grant PCIG12-GA-2012-334525), King's College London, Ministerio de Economía y Competitividad (grants CTQ 2013-40717-P, CTQ2016-76393-P and Consolider Ingenio 2010 CSD 2009-00038) and Junta de Castilla y León (Grant VA077U16). E. R. A. thanks Ministerio de Ciencia e Innovación for FPI grant (BES-2014-067776). We would like to thank Dr Silvia Gómez Coca for help with figure S2b.

Keywords: conformational analysis • flavin • laser ablation • microwave spectroscopy • ab initio calculations

- [1] J. H. J. Huck, N. M. Verhoeven, J. M. Van Hagen, C. Jakobs, M. S. Van Der Knaap, *Neuropediatrics* **2004**, *35*, 167–173.
- [2] K. Gekko, *J. Biochem.* **1981**, *90*, 1633–1641.
- [3] S. Turner, T. Senaratna, D. Touchell, E. Bunn, K. Dixon, B. Tan, *Plant Sci.* **2001**, *160*, 489–497.
- [4] R. Politi, L. Sapir, D. Harries, *J. Phys. Chem. A* **2009**, *113*, 7548–7555.
- [5] G. A. Jeffrey, H. S. Kim, *Carbohydr. Res.* **1970**, *14*, 207–216.
- [6] F. Franks, J. Dadok, S. Ying, R. L. Kay, J. R. Grigera, *J. Chem. Soc. Faraday Trans.* **1991**, *87*, 579.
- [7] G. G. Brown, B. C. Dian, K. O. Douglass, S. M. Geyer, S. T. Shipman, B. H. Pate, *Rev. Sci. Instrum.* **2008**, *79*, 1–13.
- [8] S. Mata, I. Peña, C. Cabezas, J. C. López, J. L. Alonso, *J. Mol. Spectrosc.* **2012**, *280*, 91–96.
- [9] I. Peña, S. Mata, A. Martín, C. Cabezas, A. M. Daly, J. L. Alonso, *Phys. Chem. Chem. Phys.* **2013**, *15*, 18243.
- [10] K. M. Marstokk, H. Möllendal, *J. Mol. Struct.* **1974**, *22*, 301–303.
- [11] E. Walder, A. Bauder, H. H. Günthard, *Chem. Phys.* **1980**, *51*, 223–239.
- [12] D. Christen, L. H. Coudert, R. D. Suenram, F. J. Lovas, *J. Mol. Spectrosc.* **1995**, *172*, 57–77.
- [13] D. Christen, L. H. Coudert, J. A. Larsson, D. Cremer, *J. Mol. Spectrosc.* **2001**, *205*, 185–196.
- [14] W. Caminati, *J. Mol. Spectrosc.* **1981**, *86*, 193–201.
- [15] T. J. L. Lockley, J. P. I. Hearn, A. K. King, B. J. Howard, *J. Mol. Struct.* **2002**, DOI 10.1016/S0022-2860(02)00090-X.
- [16] G. Maccaferri, W. Caminati, P. G. Favero, *J. Chem. Soc. - Faraday Trans.* **1997**, *93*, 4115–4117.
- [17] V. V. Ilyushin, R. A. Motiyenko, F. J. Lovas, D. F. Plusquellic, *J. Mol. Spectrosc.* **2008**, *251*, 129–137.
- [18] D. Loru, I. Peña, J. L. Alonso, M. Eugenia Sanz, *Chem. Commun.* **2016**, *52*, 3615–3618.
- [19] I. León, E. R. Alonso, S. Mata, C. Cabezas, M. A. Rodríguez, J.-U. Grabow, J. L. Alonso, *Phys. Chem. Chem. Phys.* **2017**, *19*, 24985–24990.
- [20] J. L. Alonso, J. C. López, in *Top. Curr. Chem.*, **2015**, pp. 335–402.
- [21] N. Gisch, T. Kohler, A. J. Ulmer, J. Muthing, T. Pribyl, K. Fischer, B. Lindner, S. Hammerschmidt, U. Zähringer, *J. Biol. Chem.* **2013**, *288*,

COMMUNICATION

WILEY-VCH

- 15654–15667.
- [22] Y. V. S. N. Murthy, V. Massey, *J. Biol. Chem.* **1995**, 270, 28586–28594.
- [23] S. Engst, P. Vock, M. Wang, J. J. P. Kim, S. Ghisla, *Biochemistry* **1999**, 38, 257–267.
- [24] W. Zhang, M. Zhang, W. Zhu, Y. Zhou, S. Wanduragala, D. Rewinkel, J. J. Tanner, D. F. Becker, *Biochemistry* **2007**, 46, 483–491.
- [25] H. S. Kim, G. A. Jeffrey, R. D. Rosenstein, *Acta Crystallogr. Sect. B Struct. Crystallogr. Cryst. Chem.* **1969**, 25, 2223–2230.
- [26] M. Dewar, E. Zebisch, E. Healy, J. Stewart, *J. Am. Chem. Soc.* **1985**, 107, 3902.
- [27] J. K. G. Watson, in *Vib. Spectra Struct. Vol. 6. A Ser. Adv.*, **1977**.
- [28] H. M. Pickett, *J. Mol. Spectrosc.* **1991**, 148, 371–377.
- [29] E. Alonso, J. Alonso, I. Peña, C. Cabezas, S. Mata, in *Proc. 71st Int. Symp. Mol. Spectrosc.*, University Of Illinois At Urbana-Champaign, Urbana, Illinois, **2016**, pp. 1–1.
- [30] E. J. Cocinero, A. Lesarri, P. Écija, F. J. Basterretxea, J. U. Grabow, J. A. Fernández, F. Castaño, *Angew. Chemie - Int. Ed.* **2012**, 51, 3119–3124.
- [31] J. L. Alonso, M. A. Lozoya, I. Peña, J. C. López, C. Cabezas, S. Mata, S. Blanco, *Chem. Sci.* **2014**, 5, 515–522.
- [32] G. A. Jeffrey, W. Saenger, *Hydrogen Bonding in Biological Structures*, Springer Berlin Heidelberg, Berlin, Heidelberg, **1991**.
- [33] G. A. Jeffrey, *An Introduction to Hydrogen Bonding*, Oxford University Press, **1997**.
- [34] P. Écija, I. Uriarte, L. Spada, B. G. Davis, W. Caminati, F. J. Basterretxea, A. Lesarri, E. J. Cocinero, *Chem. Commun.* **2016**, 52, 6241–6244.

WILEY-VCH

Accepted Manuscript